Flotation Simulation in a Cable-driven Virtual Environment - A Study with Parasailing

HyeongYeop Kang[1], **Geonsun Lee**[1], **Seongsu Kwon**[1],
Ohung Kwon[2], **Seongpil Kim**[2], **JungHyun Han**[1]
[1]Korea University, Seoul, South Korea
[2]KITECH, Ansan, South Korea
{sharm88, sh110019, tjdtn5683, jhan}@korea.ac.kr, {ohung, kspwelsh}@kitech.re.kr

ABSTRACT
This paper presents flotation simulation in a cable-driven virtual environment. For this, a virtual parasailing system was developed, where the visual stimulus was provided through a VR headset and the physical stimulus was given by wires. In order to prevent the user from moving out of the limited workspace of the cable-driven system, the visual acceleration was washout-filtered to produce the physical acceleration. In the parasailing trajectory, we focused on the stages of vertical acceleration/deceleration and conducted an experiment to identify how much gain can be applied to the visual acceleration, which makes the user feel the natural self-motion when integrated with the physical stimulus. Then, the results were tested using several types of full-course virtual parasailing. The results showed that fairly large differences between visual and physical stimuli would be accepted and different gains could be assigned depending on the user's altitudes.

ACM Classification Keywords
H.5.1 Information interfaces and presentation (e.g., HCI): Multimedia Information Systems - Artificial, augmented, and virtual realities

Author Keywords
Virtual reality; flotation simulation; flying sports; parasailing; visual gain

INTRODUCTION
Virtual reality (VR) is being used in a wide range of applications that have rarely been approachable to the general public. They include flying sports such as bungee jumping, skydiving, and parasailing. Flying sports in real life often entail accidents due to the altitudes they reach. However, simulating them in VR can provide a comparable level of enjoyment with few accidents.

CHI 2018, April 21–26, 2018, Montréal, QC, Canada.

ACM ISBN 978-1-4503-5620-6/18/04 ...$15.00.
http://dx.doi.org/10.1145/3173574.3174206

Many efforts have been made to enhance the immersion in VR sports. They include developing motion simulators. Evidence from previous studies shows that, by adding a physical stimulus in VR, users get an improved sense of self-motion. Unfortunately, every motion simulator has a limited workspace. There have been efforts to map the user's motion in a large scale virtual environment to the motion simulator. However, most studies have so far focused on horizontal movements. Surprisingly little attention has been paid to studying multiple factors that influence the illusion of self-motion in vertical motions.

A technique adopted widely in motion simulators is the washout filter, which "washes out" the position of the simulator back to its neutral position without it being noticed by the user [25]. It enables all subsequent motions to start from the same neutral position. We have developed a cable-driven virtual environment for flying sports, where the physical stimulus defined by a washout filter is given by the cable and the visual stimulus is provided through a VR headset. In order to simulate flotation in the environment, an experimental prototype for virtual parasailing was implemented. In the parasailing trajectory, we focused on the stages of vertical acceleration/deceleration and conducted an experiment to identify how the visual and physical stimuli can be naturally integrated. Then, the results were tested using several types of full-course virtual parasailing. This paper presents the key components of our flotation simulation system and the results of the experiments conducted on it.

RELATED WORK
There have been a lot of research efforts to investigate human perceptions in virtual environments, and they found that the perceived self-motion in virtual environments is often distorted. With respect to driving simulation, some studies reported that there was a misperception of speed [12, 15, 33]. Similarly, estimations of walking speed and distance during simulation were reported to be also inaccurate [2, 39]. Bruder and Steinicke [5] found that walking distances and speeds were underestimated while consumed time was overestimated in the immersive virtual environments (IVEs).

Some studies argued that failure to accurately perceive self-motion was due to the lack of sensory cues such as auditory, tactile, or vestibular cues [7, 34]. Therefore, to provide self-

motion with an improved realistic sensation, usage of multisensory cues would be recommended. Harris et al. [16] examined the contribution of visual and vestibular cues on self-motion perception in IVEs. Wright et al. [42] investigated the visual and vestibular contributions specifically on vertical self-motion perception. Berger et al. [4] conducted experiments to examine which stimulation factors were effective in increasing sense of self-motion in forward acceleration simulation.

Many efforts have been made to develop applications providing multisensory cues. Hogue et al. [17] presented the parachute simulation to improve safety and performance of smokejumper and military parachutists. It was a simple system, and the only body motion was produced by pulling a ripcord as the parachute opened. Fels et al. [8] suggested a virtual swimming interface, where the simulation gave the user a feeling of resistance and buoyancy through a rope-pulley system. Rheiner [31] provided the user with the experience of a bird in flight. The participant could control the simulator with her hands and arms, which were directly correlated to the wings and the primary feathers of the bird. Eidenberger and Mossel [6] proposed a cable-based jumping simulator composed of a head-mounted display (HMD) and a mechanical absorber system with stacked eccentric wheels. They allowed subjects to perform an indoor skydiving in an IVE. Jain et al. [20] designed a VR scuba diving simulator, where the vertical body motion was produced by a torso base (an inflatable cushion). To increase the immersion of the system, they also provided a range of senses of sight, hearing, temperature, and balance. In these works, however, the body movements were of a small distance, and proper synchronization between visual and physical stimuli has not been investigated.

While the multisensory condition has such advantages, if ill-used, some issues may emerge. For example, sensory conflicts could occur that degrade the sense of presence. Several studies investigated the visual gain to combine visual and non-visual cues optimally. Jaekl et al. [19] estimated the amount of visual motion that could be tolerated against the head movement. Powell et al. [28] and Nilsson et al. [26] found the range of visual gains which could be perceived as normal when walking on a treadmill.

To experience immersiveness in IVEs implemented with multisensory cues, many devices are required including motion simulators, HMDs, projection screens, tracking systems, and computers. This requirement inevitably restricts the user within a small workspace in the real world. To overcome this problem, several studies exploited undetectable manipulation of users. With redirected walking [29, 36] in IVEs, we can change the actual walking direction without the users noticing it and enable them to explore larger virtual environments. Matsumoto et al. [23] proposed a method for improving the effect of redirected walking by adding haptic cues. Some motion simulators tilted the seats backward below the threshold of the vestibular canal system in the acceleration motion such that users could feel prolonged linear accelerations [1, 4, 13, 14, 30]. In many motion simulators, washout filter was used for restoring the simulators back to their neutral position [11, 27]. Some studies proposed the washout filter for a flight simulator [18, 35]. They were tested with the widely-used Stewart platform [37]. Since the Stewart platform inherently offers very limited vertical motion, the washout filters were tested only on surge and pitch motions.

Previous research efforts in self-motion found that horizontal and vertical movements need to be processed differently. For example, Trutoiu et al. [40] showed that horizontal vection was perceived less convincing than vertical vection. Benson et al. [3] showed that the linear acceleration thresholds to perceive self-motion were higher for vertical motion compared to horizontal motion.

In this paper, we present a virtual parasailing system, which provides the physical stimulus through wires and the visual stimulus through an HMD. In order to provide a better sense of self-motion, we have applied gains to the visual stimulus for its optimal combination with the physical stimulus. In the open literature, however, there has been little discussion about visual gains for vertical motions, which are the primary movements for flying sports applications.

The earlier version of our cable-driven system was presented by Kim et al. [22], which was specialized for jumping motion in a gravity-reduced environment such as lunar or Martian surfaces. Our system is similar to CableRobot [24], which is also driven by wires. Whereas our system allows the user fastened in the harness to freely move their limbs and land on their feet, however, CableRobot, being a ride simulator, does not allow such motion.

VIRTUAL PARASAILING

Parasailing Model

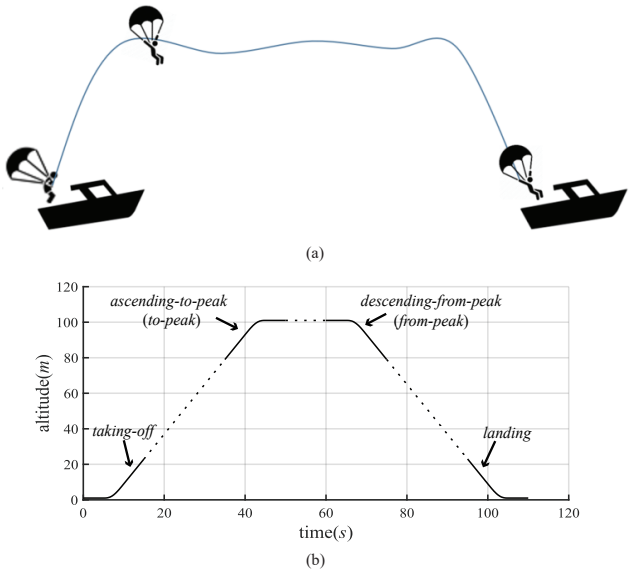

Figure 1. Parasailing altitude and the stage with prominent acceleration and deceleration.

This paper reports a study with a popular recreational activity, parasailing, also known as parakiting. The harness fastening

a person is attached to a parasail, which is a large parachute, and is also connected to a boat through a rope. When the boat drives off, the parasail and the person are carried into the air, and the rope controls the height of parasail. Figure 1-(a) depicts a typical trajectory of parasailing.

In our study, we assume that the boat deck is $1m$ above the water surface and the maximum flight height is $100m$, i.e., the user can reach the peak at the altitude of $101m$ above the water surface. We also assume that the longitudinal or horizontal motion of the parasail is made with a constant velocity. Focusing on the vertical motion, we are interested in the stages with "prominent acceleration and deceleration." Figure 1-(b) illustrates our model of time-varying altitudes with four stages of interest: *taking-off* (from the boat deck), *ascending-to-peak* (reaching the elevation of $101m$), *descending-from-peak*, and *landing* (on the boat deck). For the sake of simplicity, ascending-to-peak will be shortened to *to-peak*, and descending-from-peak will be *from-peak*.

Figure 2-(a) shows the close-up view of the *taking-off* stage (left) and the vertical acceleration for the stage (in a blue curve on the right). Based on the empirical data, 15 seconds are assigned to *taking-off*, and it is partitioned into three sub-stages: 5 seconds with zero velocity, 5 seconds with acceleration, and 5 seconds with a constant non-zero velocity.

Similar discussions can be made for the other three stages. For example, *to-peak* shown in Figure 2-(b) is composed of 5 seconds with a constant non-zero velocity, 5 seconds with deceleration, and 5 seconds with zero velocity. Figure 2-(c) and -(d) show the stages of *from-peak* and *landing*, respectively.

The first 5 seconds of *to-peak* have the same constant velocity as that of the last 5 seconds of *taking-off*. This applies between every pair of consecutive stages, and the period between them (corresponding to the dotted line in Figure 1-(b)) has the constant velocity. The magnitude of deceleration in *to-peak* is identical to that of acceleration in *taking-off* so that the vertical velocity of the parasail remains zero while hovering at the peak, the altitude of $101m$. Similar discussions can be made between *from-peak* and *landing*.

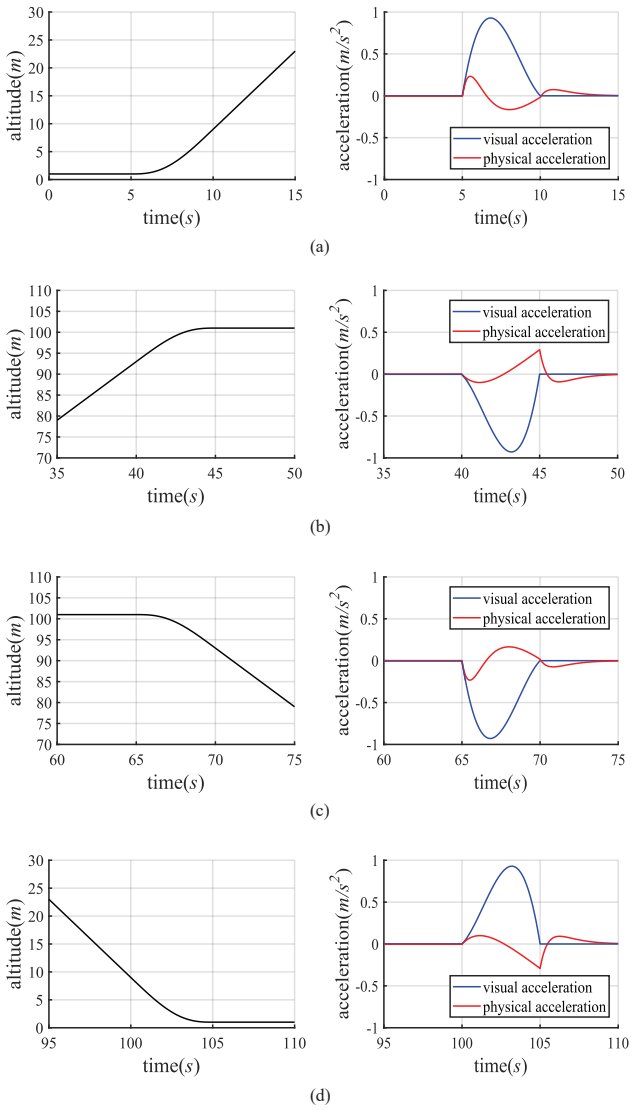

Figure 2. Altitudes and visual/physical accelerations. (a) *Taking-off*. (b) *To-peak*. (c) *From-peak*. (d) *Landing*.

Cable-driven System and Washout Filter

As a motion platform for virtual parasailing, we use a cable-driven system shown in Figure 3. It has four wires, each of which connects a drum winch and the harness through a pulley. A drum winch is equipped with a 12KW motor. Within the workspace of $4m \times 4m \times 4m$, the wires driven by the drum winches can freely move the user wearing the harness. In the current study focusing on the vertical acceleration/deceleration, however, the user is lifted only up and down.

Obviously, the workspace of the cable-driven system is too small to provide the real trajectory of parasailing. In order to overcome this limitation, we resort to a *washout filter*, which has been widely used for enabling a motion platform to provide various trajectories [11, 27].

Consider the stage of *taking-off* presented in Figure 2-(a). In virtual parasailing, the acceleration depicted in the blue curve is used to generate the visual stimulus, i.e., the first-person's view of parasailing scene. In this sense, it is called *visual acceleration* and denoted as α_v. On the other hand, the *physical acceleration* to be provided by the cable-driven system is denoted as α_p. In the current study, we use a second-order high-pass filter for the washout filter. It takes α_v as input and returns α_p:

$$\alpha_p = \frac{s^2}{s^2 + 2\zeta\omega_n s + \omega_n^2}\alpha_v, \quad s = \frac{2}{t_s}\left(\frac{1-p^{-1}}{1+p^{-1}}\right) \qquad (1)$$

where s denotes the Laplace operator, ζ is the damping ratio, ω_n represents the natural frequency, t_s is the sampling interval ($2ms$ in the current implementation), and p is the shift operator, also called discrete-time operator [10].

The physical acceleration (α_p) computed using Equation (1) is depicted in a red curve in Figure 2-(a). It starts to increase

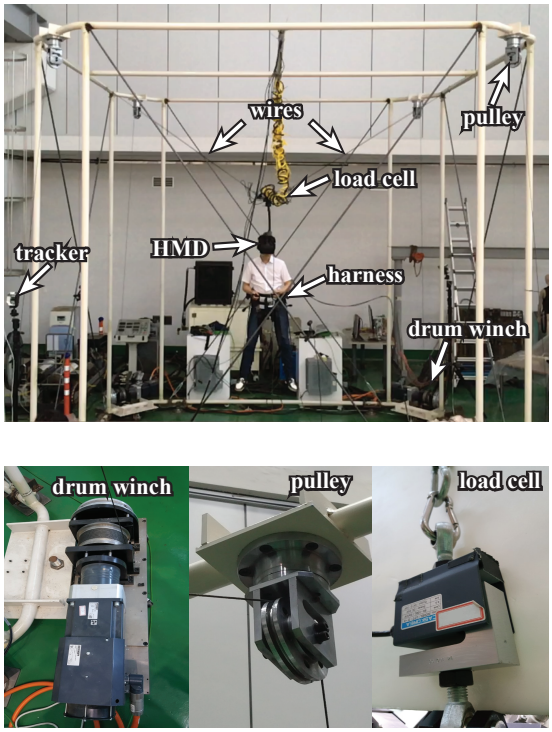

Figure 3. Cable-driven system and its components.

simultaneously with the visual acceleration (α_v) and reaches the peak of $0.24m/s^2$, which is far smaller than that of α_v ($0.95m/s^2$). Then, it decreases, falls below zero, and is eventually washed out to zero after about 10 seconds. It is important to note that α_p restores the user to the initial position in the cable-driven system. We call this *neutral position*. The washout filter not only prevents the user from moving out of the workspace but also makes the motion of every stage start from the same neutral position. In the current implementation, the neutral position of the harness is $2.8m$ high, and the vertical range of motion is $\pm 0.7m$ from the neutral position. The physical accelerations for the stages of *to-peak*, *from-peak*, and *landing* are also computed using Equation (1). They are illustrated with red curves in Figure 2-(b), -(c), and -(d).

In the cable-driven system, the force needed to lift the user up and down is determined as follows:

$$f = k_1 mg + k_2(p_d - p_m) \quad (2)$$

where k_1 and k_2 are the control coefficients, m is the user's mass, g is the gravitational acceleration, and p_d and p_m represent the "desired" and "measured" position vectors, respectively. Using the encoders embedded in the drum winches, the kinematic displacement of the end-effector (harness) is measured. It provides p_m for Equation (2). On the other hand, p_d is computed by integrating α_p twice.

We adopt a proportional-integral-derivative (PID) control. As can be found in Figure 3, a *load cell* is located between the harness and a pulley. It senses the tension of a wire every $2ms$. Let t_i denote the tension of the i-th wire. Once f is computed in Equation (2), it is distributed to four wires of the cable-driven system through a kinematic transformation. Let f_i denote the force assigned to the i-th wire. The PID controller keeps the tension error, i.e., $f_i - t_i$, smaller than a threshold.

Immersive Virtual Environment

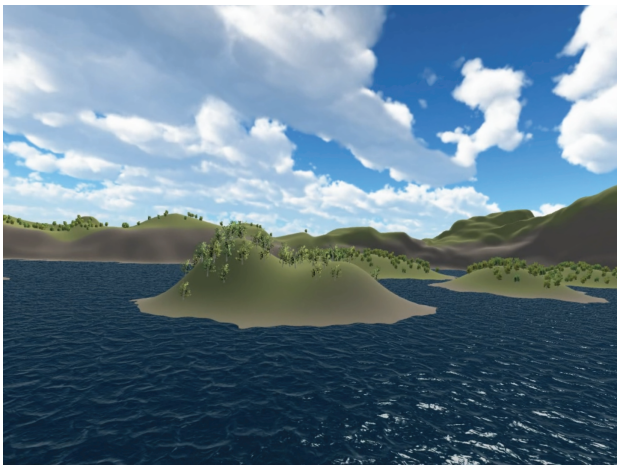

Figure 4. Lake scenery for parasailing.

We created a common parasailing scene used for experiments. As shown in Figure 4, it was a lake with small islands and surrounding mountains. The ripple effects were added to the lake surface to increase the realism. The scene was created and rendered using the Unity game engine and was viewed through an HMD, Oculus Rift Consumer Version 1, with the resolution of 1080×1200 per eye, 110° field of view, and 90Hz refresh rate. We also used the motion controller, Oculus Touch, not only for tracking and displaying the user's hands but also for user's answering the post-experiment questions. To track both HMD and motion controller, two positional trackers were installed near the corners of the cable-driven system. Multiple fans were used to simulate wind blown into the user.

OVERVIEW OF EXPERIMENTS

In our study, the visual stimulus is provided through HMD and the physical stimulus is given by the cable-driven system. If the visual and physical stimuli are mismatched, the user may suffer from a sensory conflict and the sense of presence would be decreased. The goal of our experiments is to find how the visual and physical stimuli can be naturally integrated.

We made two experiments. The goal of the first one (henceforth, E1 standing for Experiment 1) was to estimate the acceptable range of *gains* for visual acceleration, which we simply call *visual gains*. When the visual gain is one, the visual and physical accelerations follow the blue and red curves, respectively, presented in Figure 2. If the gain is three, for example, the visual acceleration is scaled by three and the scene rendered using it is displayed in the HMD screen whereas the physical acceleration in Figure 2 remains unchanged. The goal of the second experiment (henceforth, E2 standing for

Experiment 2) was to prove the range of natural gains estimated in E1, expecting that virtual parasailing with natural gains would provide a higher degree of presence than that with out-of-range gains.

In both E1 and E2, the same group of thirteen subjects (10 males and 3 females) participated. They were undergraduate and graduate students, and their ages were between 22 and 31 (M=23.92 and SD=2.23). All subjects had a normal or corrected-to-normal vision, and they had no history of the neural or vestibular disorder. Eleven subjects had experiences in playing 3D games, twelve had experiences in watching 3D movies, and thirteen had experiences in wearing HMD.

EXPERIMENT 1

The goal of E1 is to estimate the range of visual gains, which can make the user feel the natural self-motion when integrated with physical stimulus provided by the cable-driven system.

Method and Procedure

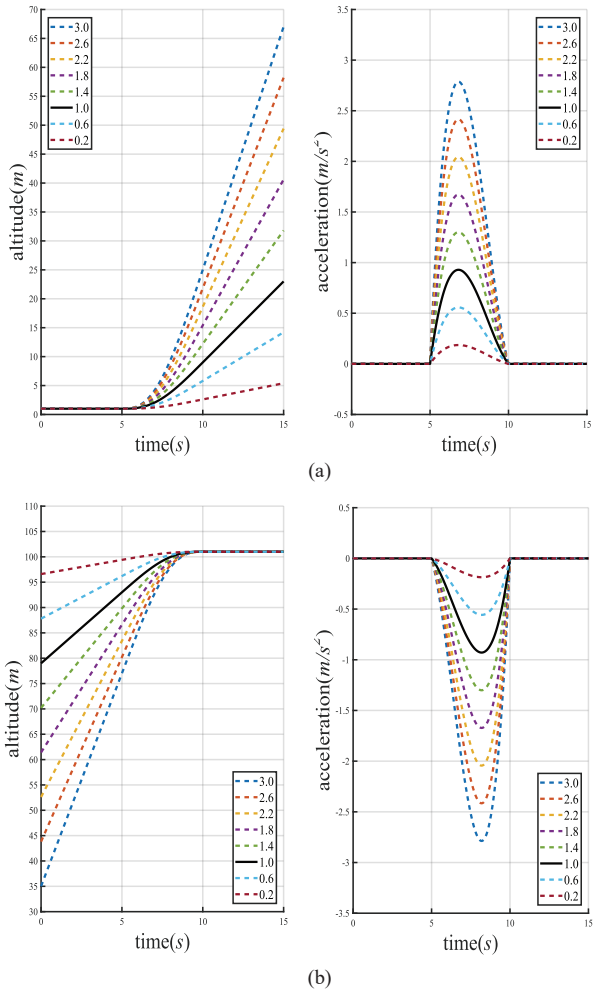

Figure 5. Gain-applied visual accelerations and the altitudes determined by them. The black solid curves correspond to the visual accelerations and altitudes presented in Figure 2. (a) *Taking-off*. (b) *To-peak*.

As illustrated in Figure 1-(b), we focused on four stages with prominent acceleration and deceleration: *taking-off*, *to-peak*, *from-peak*, and *landing*. For each stage, the physical acceleration was fixed to the red curve shown in Figure 2. Through a pilot test, the visual gain was restricted to the range of $[0.2, 3.0]$ in steps of 0.4, i.e., we had eight gain values in total. Figure 5 shows the gain-applied accelerations and the resulting altitudes in the visual stimulus for *taking-off* and *to-peak*. The visual gains are applied for *from-peak* and *landing* in the same fashion. On the other hand, the longitudinal or horizontal motion (provided only in the visual stimulus) was made with a constant velocity, $4m/s$, for all stages.

It is obvious that the final altitude of *taking-off* depends on the visual gain. In *to-peak*, however, the final altitude is fixed to $101m$, and therefore the initial altitude is determined by the visual gain. Similarly, the visual gain for *from-peak* determines its final altitude whereas the visual gain for *landing* determines its initial altitude. Using such initial and final altitudes in a stage, the trajectory of the stage was pre-computed for the experiment.

The four stages were experimented one by one. For a stage, we used a block composed of 8 trials, each with a different gain, and the subject went through 10 blocks. The order of trials was counterbalanced between blocks. A subject did 80 trials per stage and 320 (80×4) trials in total.

A stage was composed of three sub-stages (5 seconds with a constant velocity, 5 seconds with acceleration or deceleration, and 5 seconds with another constant velocity). Figure 6-(a) and -(b) show the visual/physical stimuli of the first and second sub-stages, respectively, in *taking-off*. A trial consumed 15 seconds. When a trial was done, the HMD screen faded out to black and the subject was instructed to choose whether the visual stimulus was “too slow,” “natural,” or “too fast” compared to the physical stimulus. Figure 6-(c) shows the instruction billboard. The subject made a choice with Oculus Touch.

step	time(min)
instructions & informed consent	10
trial ride	5
training for experiment	5
break	10
pre-SSQ for stage 1	1
experiment with stage 1	57
post-SSQ for stage 1	1
break	10
pre-SSQ for stage 2	1
experiment with stage 2	57
post-SSQ for stage 2	1
break	10
pre-SSQ for stage 3	1
experiment with stage 3	57
post-SSQ for stage 3	1
break	10
pre-SSQ for stage 4	1
experiment with stage 4	57
post-SSQ for stage 4	1

Table 1. Steps for E1. The order of stages was counterbalanced between subjects. For example, stage 1 was not necessarily *taking-off*.

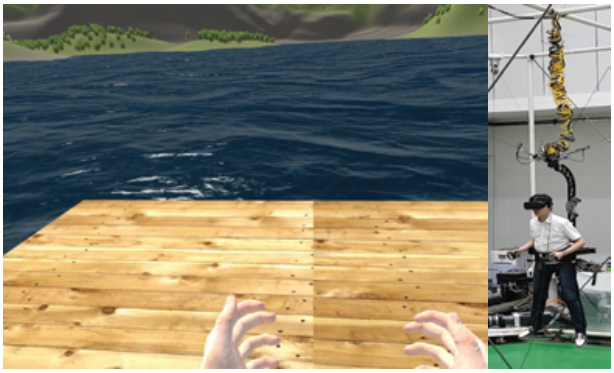

(a)

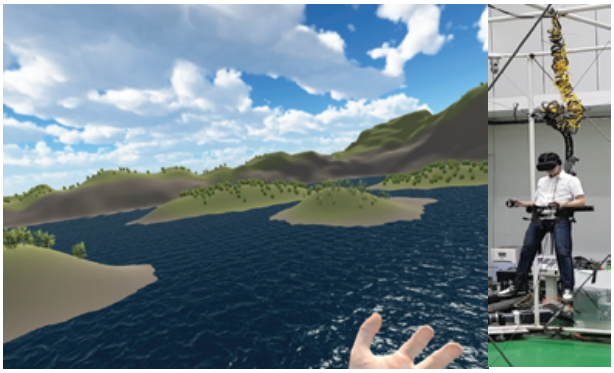

(b)

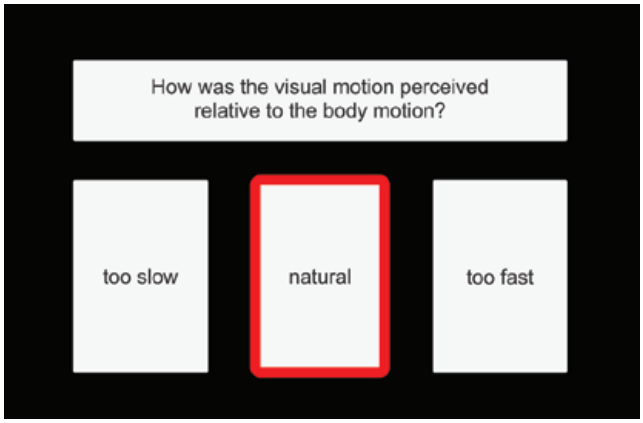

(c)

Figure 6. Experiment for *taking-off*. (a) The first sub-stage of five seconds with zero velocity. (b) The second sub-stage of five seconds with acceleration. (c) Instruction billboard.

The steps of E1 are enumerated in Table 1 with the elapsed time on each step. After a brief explanation of the experiment, each subject signed the consent form. Then, wearing the harness and HMD, the subject took a trial ride for full-course parasailing from *taking-off* to *landing*. For this, the gain was set to one, i.e., the visual and physical accelerations follow the blue and red curves, respectively, in Figure 2.

Then, the subject was trained for the experiment. Each of the four stages was presented for 15 seconds with a randomly-assigned gain, and the subject was instructed how to choose among "too slow," "natural," and "too fast" using Oculus Touch.

After taking a ten-minute break, the four stages were experimented one by one. The order of stages was counterbalanced between subjects. The experiment for a stage consisted of 10 blocks. A block took about three minutes, and a three-minute break was between blocks. Right before and after the experiment for a stage, the subject filled the Simulator Sickness Questionnaire (SSQ) [21]. The experiment for a stage took about an hour. A ten-minute break was between stages. The entire experiment took almost five hours. The subjects were allowed to take their own breaks at any time, but no such break was taken. A subject was offered 50 USD for participation.

Results and Discussion

The experiment result is presented in Figure 7, where the x-axis is for the visual gain and the y-axis shows the probability of taking the gain-applied visual stimulus as natural. The data are fitted with a Gaussian, where μ and σ denote the mean and standard deviation, respectively. Table 2 lists the parameters of the Gaussians. In each stage, μ is taken as the most natural gain, and the range of natural gains is defined by $\mu \pm \sigma$, accounting for 68% of the natural judgements.

It is interesting to find that the most natural gain is far greater than 1.0 for every stage. This implies that a visual stimulus can be taken as natural even though it is fairly faster than the physical stimulus. In the studies of horizontal translation [26, 28], similar results were reported that people felt natural when the visual stimulus was faster than the physical stimulus.

A one-way analysis of variance (ANOVA) test revealed that there were significant differences between the distributions of natural gains in four stages ($F(3, 1945) = 159.57, p < 0.05$). The post-hoc analysis, Tukey-Kramer method, suggested that there was no significant difference between *to-peak* and *from-peak* but all the other pairs of stages showed significant differences.

Table 2 shows that the most natural gains (μ) for *to-peak* and *from-peak* are much greater than those for *taking-off* and *landing*. This implies that the visual stimulus at a higher altitude can be made faster. It is compatible with what Festl et al. [9] found: Perceiving ego-accelerations depends on visual scale of the scene provided through depth cues. As the user's altitude increases, the objects on the ground or lake surface provide a smaller visual scale, leading to less convincingness of self-motion. Therefore, the larger visual gain can be used at the higher altitude.

In addition, observe that μ in *landing* is smaller than that of *taking-off*. This implies that subjects are more sensitive to landing than taking off.

We also investigated whether the repeated trials made the users get used to the virtual environments and eventually affected their choices. For the experiment of each stage, we extracted the first five blocks, collecting a set of 20 (5×4)

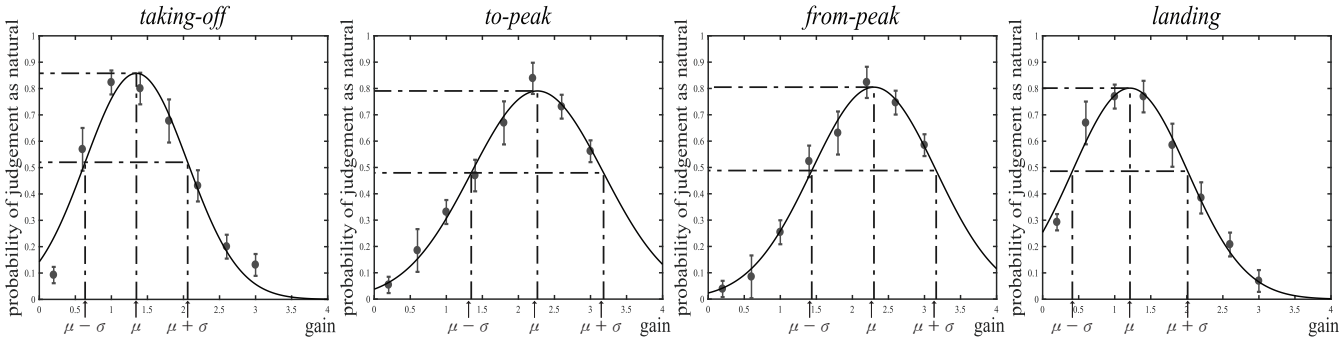

Figure 7. For each stage of *taking-off*, *to-peak*, *from-peak*, and *landing*, the mean (μ) and standard deviation (σ) are computed for eight visual gains, and the data are fitted with a Gaussian.

stage	μ	σ	$\mu \pm \sigma$	R^2
taking-off	1.361	0.681	$[0.680, 2.042]$	0.941
to-peak	2.261	0.907	$[1.354, 3.168]$	0.988
from-peak	2.298	0.859	$[1.439, 3.157]$	0.992
landing	1.260	0.726	$[0.534, 1.986]$	0.942

Table 2. The parameters of the Gaussians obtained in Figure 7. R^2 denotes the coefficient of determination.

blocks. Similarly, we extracted the last five blocks for each stage, collecting another set of 20 blocks. The ANOVA test revealed that there was no significant difference between two sets ($F(1,1947) = 0.23, p > 0.05$). While a block took around three minutes, the break between blocks also lasted three minutes. These breaks may have prevented the subjects from getting used to the virtual environments.

stage	pre-SSQ		post-SSQ		F(1,24)
	μ	σ	μ	σ	p
taking-off	1.461	1.942	1.923	2.178	0.574
to-peak	1.692	1.548	2.308	1.751	0.351
from-peak	1.154	1.281	2.000	2.160	0.236
landing	2.000	2.646	2.692	2.136	0.470

Table 3. SSQ analysis.

The SSQ answers were analyzed using the method proposed by [32, 38]. See Table 3 for the results. There were no significant differences.

EXPERIMENT 2

In E1, the most natural gain, μ, and the natural-gain range, $[\mu - \sigma, \mu + \sigma]$, were identified for each of four stages. E2 tested these with full-course parasailing. Our hypothesis was two-folded: (1) Parasailing with the most natural gain would provide the user with the strongest sense of presence. (2) If the gains were out of the natural-gain range, the sense of presence would be decreased.

Method and Procedure

For E2, we designed five types of parasailing. No physical stimulus was provided for the first one (**visual-only**), but both of visual and physical stimuli were provided for all the others.

- **visual-only**: The subject was given the visual stimulus based on the altitudes presented in Figure 1-(b), but no physical stimulus was provided by the cable-driven system.
- **standard**: The visual gain was set to 1.0 for every stage.
- **natural**: For each stage, the most natural gain identified in E1 was applied.
- **slow-to-quick**: The gain for *taking-off* was below the natural-gain range whereas that for *to-peak* was above the range. As can be observed in Figure 8-(a), this combination made *taking-off* "slow" and *to-peak* "quick." In the same manner, the gain for *from-peak* was below the natural-gain range whereas that for *landing* was above the range.
- **quick-to-slow**: The gain for *taking-off* was above the natural-gain range, making *taking-off* "quick." In contrast, the gain for *to-peak* was below the range, making *to-peak* "slow." See Figure 8-(b). In the same manner, the gain for *from-peak* was above the natural-gain range whereas that for *landing* was below the range.

Table 4 shows the visual gains used for five types of parasailing.

parasailing type	visual gain			
	taking-off	*to-peak*	*from-peak*	*landing*
visual-only	1.000	1.000	1.000	1.000
standard	1.000	1.000	1.000	1.000
natural	1.361	2.261	2.298	1.260
slow-to-quick	0.230	3.656	0.979	2.433
quick-to-slow	2.464	0.871	3.619	0.200

Table 4. Parasailing types and their visual gains. The visual gains for natural, slow-to-quick, and quick-to-slow are determined based on Table 2.

step	time(min)
instructions & informed consent	10
initial setup	5
experiment with parasailing type 1	5.5
SUS questionnaire	1
break	10
experiment with parasailing type 2	5.5
SUS questionnaire	1
break	10
experiment with parasailing type 3	5.5
SUS questionnaire	1
break	10
experiment with parasailing type 4	5.5
SUS questionnaire	1
break	10
experiment with parasailing type 5	5.5
SUS questionnaire	1

Table 5. Steps for E2. The order of parasailing types was counterbalanced between subjects. For example, type 1 was not necessarily visual-only.

E2 was conducted with the same subjects participating in E1 and was a week separated from E1. The steps of E2 are enumerated in Table 5 with the elapsed time on each step. The five types of parasailing were experimented one by one. The order of types was counterbalanced between subjects, and the subjects were not aware of which type they experimented with. For a type, the full-course parasailing was repeated three times: As soon as the subject landed on the boat deck, she started to take off. The time taken by a full-course parasailing was fixed to 110 seconds, and therefore experimenting with a type of parasailing took 330 seconds (5.5 minutes). For presence evaluation, the subject completed a Slater-Usoh-Steed (SUS) [41] questionnaire after finishing a parasailing type. A ten-minute break was given between parasailing types. The entire experiment took about 1.5 hours. A subject was offered 20 USD for participation.

Results and Discussion

	mean	*standard deviation*
visual-only	14.846	5.984
standard	22.385	3.969
natural	29.923	4.406
slow-to-quick	20.385	3.070
quick-to-slow	21.769	6.521

Table 6. SUS scores in E2.

Table 6 shows the SUS scores for five parasailing types. As expected, **natural** showed the highest score while **visual-only** showed the lowest score. The results of the SUS questionnaire for each type were found to be normally distributed according to Shapiro-Wilk test at the 5% level. The ANOVA test revealed that there were significant differences between the SUS scores ($F(4,60) = 15.42$, $p < 0.01$). Through the post-hoc analysis, Tukey-Kramer method, we found that the SUS score of **natural** was significantly different from the other four types. The SUS score of **visual-only** was also significantly different from the others. On the other hand, there were no significant differences between **standard**, **slow-to-quick**, and **quick-to-slow**.

It is worth discussing a few issues regarding E2 implementation. Recall that, as discussed with Figure 1-(b), the period between two consecutive stages has the same constant velocity. Unfortunately, this does not hold for **natural**, **slow-to-quick**, and **quick-to-slow** because different magnitudes of acceleration/deceleration are applied in the stages. Figure 8-(c) shows the case of **natural**, where the visual gain for *taking-off* (1.361) is different from that for *to-peak* (2.261). The sequel to these assignments is as follows: The visual acceleration for *taking-off* (denoted by α_1) and the visual deceleration for *to-peak* (denoted by α_2) have different magnitudes; The final velocity of *taking-off* (v_1) and the initial velocity of *to-peak* (v_2) are different; The period between *taking-off* and *to-peak* cannot be assigned a constant velocity.

Our solution to this problem was simple: v_1 and v_2 were linearly interpolated for the period. The same solution was applied between *from-peak* and *landing*. Then, the entire trajectory was computed and used for rendering. Observe that, in Figure 8-(c), the trajectory between two stages is not a line but a curve because the velocity is not constant. Figure 9 compares the altitude graphs of five parasailing types. Observe that the trajectory between ascending/descending stages is a line in **visual-only** and **standard** whereas that is a curve in **natural**, **slow-to-quick**, and **quick-to-slow**.

Figure 9 also shows that, in **natural**, **slow-to-quick**, and **quick-to-slow**, we reach the peak (at the altitude of $101m$) earlier than in **visual-only** and **standard**. Such a short elapsed time for reaching the peak made us choose only **slow-to-quick** and **quick-to-slow** out of all possible combinations. Suppose that, for example, *taking-off* and *to-peak* were assigned the visual gains above the natural-gain range. Such a **quick-to-quick** parasailing type takes shorter to reach the peak, and as illustrated in Figure 8-(d), the cable-driven motion for *to-peak* would start before the user in the stage of *taking-off* is restored to the neutral position. This is not compatible with the washout filter.

FIELD OBSERVATIONS

After the experiments, the subjects were asked if they had sensory conflict caused by the washout filter, i.e., if they perceived that they were restored back to the neutral position after being moved up or down. Nobody experienced this conflict, which indicated that our washout filter worked for the vertical motion.

We also conducted an interview to collect general comments. In our virtual parasailing system, the vertical velocity of the parasail remains zero while hovering at its peak altitude of $101m$. A subject complained that it was boring and proposed that we add a small motion at the peak. Another subject proposed that we increase the wind velocity and decrease the temperature while ascending and the reverse while descending.

Our harness has evolved for many years. Its first prototype applied pressure to the upper thigh and groin of the user. This problem was largely resolved by embedding air cushions into the harness, but heavy users still experienced discomfort. Thus a strap was attached to the harness for each foot so as to distribute the user's weight across the harness and both feet.

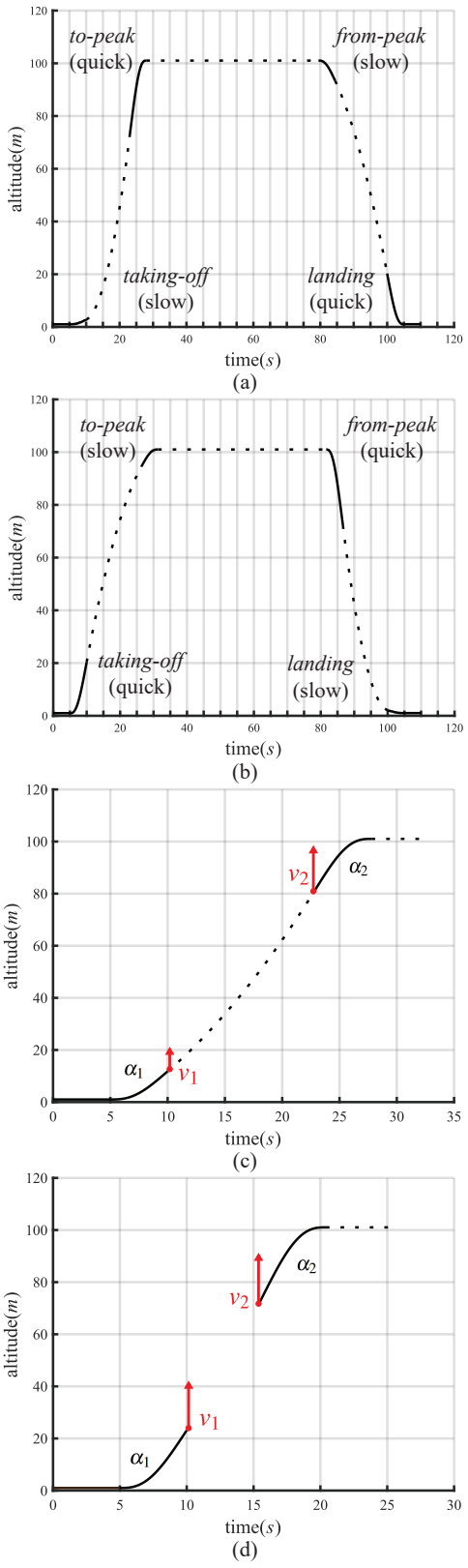

Figure 8. Combinations of gains assigned to the stages. For each stage of 15 seconds, only the 5-second sub-stage in the middle is depicted in a solid curve. (a) Slow-to-quick. (b) Quick-to-slow. (c) Interpolation of velocities (in red vectors) and resulting altitudes (in dotted curve) for the type of "natural." (d) Quick-to-quick.

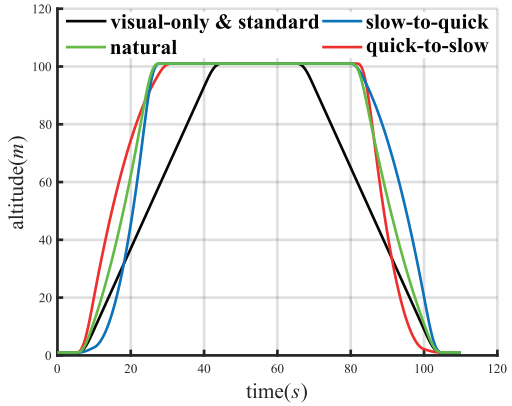

Figure 9. The altitude graphs of five types of parasailing.

During the experiments, few participants complained about the harness.

As our cable system was set up in an off-campus facility, we were able to recruit only a limited number of students living near the location, and consequently E1 and E2 were conducted with the same subjects. It would be better if they were made with different subjects. However, E1 and E2 were separated by a week, and we think that such a separation would prevent the subjects from getting used to the cable system.

CONCLUSION

We presented virtual parasailing, where the visual stimulus is provided through a VR headset and the physical stimulus is given by a cable-driven system. In order to prevent the user from moving out of the limited workspace of the cable-driven system, the visual acceleration is washout-filtered to produce the physical acceleration. Then, an experiment was conducted to identify how much gain can be applied to the visual acceleration, which makes the user feel the natural self-motion when integrated with the physical stimulus. The results were tested using several types of full-course virtual parasailing. The results showed that fairly large differences between visual and physical stimuli would be accepted and different gains could be assigned depending on the user's altitudes.

Our research results can be applied to various instances of flotation simulation with jumping and free-fall motions. Good candidates include skydiving and bungee jumping, where the dominant motions are made along the vertical direction. Note that our cable-driven system can freely move the manned harness in any direction within the workspace. Therefore, free-flying extreme sports such as paragliding and wingsuit flying could also be simulated with appropriate extensions of acceleration/deceleration controls for surge and sway motions. Further investigations will be made for such extensions.

Our experiment also has limitations. A notable one is that no haptic stimulus was provided for the user's feet. In the real-world parasailing, people first stand on the boat deck and

then take off. In our experiment, however, the user started *taking-off* from the neutral position, i.e., from the state of being suspended in air. Consequently, no haptic feedback was provided on the feet. It is well known that haptic cues have a huge impact on identifying visual gains [36]. If appropriate haptic feedback were provided for both *taking-off* and *landing* in our experiments, substantially different results would be obtained. Integrating the haptic cue into the cable-driven system is an area of potential future work.

ACKNOWLEDGMENTS

This work was supported by the National Research Foundation of Korea (NRF) Grant funded by the Korea government (No. NRF-2016R1A2B3014319 and NRF-2017M3C4A7066316)

REFERENCES

1. David Allerton. 2009. *Principles of flight simulation*. John Wiley & Sons.
2. Tom Banton, Jeanine Stefanucci, Frank Durgin, Adam Fass, and Dennis Proffitt. 2006. The perception of walking speed in a virtual environment. *Perception* 14, 4 (2006).
3. AJ Benson, MB Spencer, and JR Stott. 1986. Thresholds for the detection of the direction of whole-body, linear movement in the horizontal plane. *Aviation, space, and environmental medicine* (1986).
4. Daniel R Berger, Jörg Schulte-Pelkum, and Heinrich H Bülthoff. 2010. Simulating believable forward accelerations on a stewart motion platform. *ACM Transactions on Applied Perception (TAP)* 7, 1 (2010), 5.
5. Gerd Bruder and Frank Steinicke. 2014. Threefolded motion perception during immersive walkthroughs. In *Proceedings of the 20th ACM symposium on virtual reality software and technology*. ACM, 177–185.
6. Horst Eidenberger and Annette Mossel. 2015. Indoor skydiving in immersive virtual reality with embedded storytelling. In *Proceedings of the 21st ACM Symposium on Virtual Reality Software and Technology*. ACM, 9–12.
7. Leonard Evans. 1970. Speed estimation from a moving automobile. *Ergonomics* 13, 2 (1970), 219–230.
8. Sidney Fels, Steve Yohanan, Sachiyo Takahashi, Yuichiro Kinoshita, Kenji Funahashi, Yasufumi Takama, and Grace Tzu-Pei Chen. 2005. User experiences with a virtual swimming interface exhibit. In *International Conference on Entertainment Computing*. Springer, 433–444.
9. Freya Festl, Fabian Recktenwald, Chunrong Yuan, and Hanspeter A Mallot. 2012. Detection of linear ego-acceleration from optic flow. *Journal of vision* 12, 7 (2012), 10–10.
10. Gene F Franklin, J David Powell, Abbas Emami-Naeini, and J David Powell. 1994. *Feedback control of dynamic systems*. Vol. 3. Addison-Wesley Reading, MA.
11. Peter R Grant and Lloyd D Reid. 1997. Motion washout filter tuning: Rules and requirements. *Journal of Aircraft* 34, 2 (1997), 145–151.
12. John A Groeger, Oliver MJ Carsten, E Blana, and A Hamish Jamson. 1999. Speed and distance estimation under simulation conditions. *Vision in vehicles* 7 (1999), 291–299.
13. EL Groen and W Bles. 2004. How to use body tilt for the simulation of linear self motion. *Journal of Vestibular Research* 14, 5 (2004), 375–385.
14. Eric L Groen, Mario SV Valenti Clari, and RJAW Hosman. 2000. Psychophysical thresholds associated with the simulation of linear acceleration. In *Proceedings of the AIAA Modeling and Simulation Technologies Conference, Denver (CO), August*. 14–17.
15. Sauli Häkkinen. 1963. *Estimation of distance and velocity in traffic situations*. Työterveyslaitos.
16. Laurence R Harris, MR Jenkin, D Zikovitz, Fara Redlick, P Jaekl, UT Jasiobedzka, HL Jenkin, and Robert S Allison. 2002. Simulating self-motion I: Cues for the perception of motion. *Virtual Reality* 6, 2 (2002), 75–85.
17. Jeffrey R Hogue, R Wade Allen, Jerry MacDonald, Cliff Schmucker, Steve Markham, and Arvid Harmsen. 2001. Virtual reality parachute simulation for training and mission rehearsal. *AIAA-2001-2061* (2001), 381–388.
18. Jacob A Houck, Robert J Telban, and Frank M Cardullo. 1999. Developments in human centered cueing algorithms for control of flight simulator motion systems. *American Institute of Aeronautics and Astronautics, AIAA-99-4328* (1999).
19. PM Jaekl, MR Jenkin, and Laurence R Harris. 2005. Perceiving a stable world during active rotational and translational head movements. *Experimental brain research* 163, 3 (2005), 388–399.
20. Dhruv Jain, Misha Sra, Jingru Guo, Rodrigo Marques, Raymond Wu, Justin Chiu, and Chris Schmandt. 2016. Immersive terrestrial scuba diving using virtual reality. In *Proceedings of the 2016 CHI Conference Extended Abstracts on Human Factors in Computing Systems*. ACM, 1563–1569.
21. Robert S Kennedy, Norman E Lane, Kevin S Berbaum, and Michael G Lilienthal. 1993. Simulator sickness questionnaire: An enhanced method for quantifying simulator sickness. *The international journal of aviation psychology* 3, 3 (1993), 203–220.
22. MyoungGon Kim, Sunglk Cho, Tanh Quang Tran, Seong-Pil Kim, Ohung Kwon, and JungHyun Han. 2017. Scaled Jump in Gravity-Reduced Virtual Environments. *IEEE Transactions on Visualization and Computer Graphics* 23, 4 (2017), 1360–1368.
23. Keigo Matsumoto, Yuki Ban, Takuji Narumi, Tomohiro Tanikawa, and Michitaka Hirose. 2016. Curvature manipulation techniques in redirection using haptic cues. In *3D User Interfaces (3DUI), 2016 IEEE Symposium on*. IEEE, 105–108.

24. Philipp Miermeister, Maria Lächele, Rainer Boss, Carlo Masone, Christian Schenk, Joachim Tesch, Michael Kerger, Harald Teufel, Andreas Pott, and Heinrich H Bülthoff. 2016. The cablerobot simulator large scale motion platform based on cable robot technology. In *Intelligent Robots and Systems (IROS), 2016 IEEE/RSJ International Conference on*. IEEE, 3024–3029.

25. MA Nahon, LD Reid, and J Kirdeikis. 1992. Adaptive simulator motion software with supervisory control. *Journal of Guidance, Control, and Dynamics* 15, 2 (1992), 376–383.

26. Niels Christian Nilsson, Stefania Serafin, and Rolf Nordahl. 2014. Establishing the range of perceptually natural visual walking speeds for virtual walking-in-place locomotion. *IEEE transactions on visualization and computer graphics* 20, 4 (2014), 569–578.

27. Russell V Parrish, James E Dieudonne, and Dennis J Martin Jr. 1975. Coordinated adaptive washout for motion simulators. *Journal of aircraft* 12, 1 (1975), 44–50.

28. Wendy Powell, Brett Stevens, Steve Hand, and Maureen Simmonds. 2011. Blurring the boundaries: The perception of visual gain in treadmill-mediated virtual environments. In *3rd IEEE VR 2011 Workshop on Perceptual Illusions in Virtual Environments*.

29. Sharif Razzaque, Zachariah Kohn, and Mary C Whitton. 2001. Redirected walking. In *Proceedings of EUROGRAPHICS*, Vol. 9. Manchester, UK, 105–106.

30. Gilles Reymond, Jacques Droulez, and Andras Kemeny. 2002. Visuovestibular perception of self-motion modeled as a dynamic optimization process. *Biological Cybernetics* 87, 4 (2002), 301–314.

31. Max Rheiner. 2014. Birdly an attempt to fly. In *ACM SIGGRAPH 2014 Emerging Technologies*. ACM, 3.

32. Bernhard E Riecke, Jörg Schulte-Pelkum, Marios N Avraamides, Markus Von Der Heyde, and Heinrich H Bülthoff. 2006. Cognitive factors can influence self-motion perception (vection) in virtual reality. *ACM Transactions on Applied Perception (TAP)* 3, 3 (2006), 194–216.

33. Santo Salvatore. 1969. *VELOCITY SENSING—COMPARISON OF FIELD AND LABORATORY METHODS*. Technical Report.

34. George Semb. 1969. Scaling automobile speed. *Attention, Perception, & Psychophysics* 5, 2 (1969), 97–101.

35. Raphael Sivan, Jehuda Ish-Shalom, and Jen-Kuang Huang. 1982. An optimal control approach to the design of moving flight simulators. *IEEE Transactions on Systems, Man, and Cybernetics* 12, 6 (1982), 818–827.

36. Frank Steinicke, Gerd Bruder, Jason Jerald, Harald Frenz, and Markus Lappe. 2010. Estimation of detection thresholds for redirected walking techniques. *IEEE transactions on visualization and computer graphics* 16, 1 (2010), 17–27.

37. Doug Stewart. 1965. A platform with six degrees of freedom. *Proceedings of the institution of mechanical engineers* 180, 1 (1965), 371–386.

38. Evan A Suma, Seth Clark, David Krum, Samantha Finkelstein, Mark Bolas, and Zachary Warte. 2011. Leveraging change blindness for redirection in virtual environments. In *Virtual Reality Conference (VR), 2011 IEEE*. IEEE, 159–166.

39. AEI Thurrell, A Pelah, and HK Distler. 1998. The influence of non-visual signals of walking on the perceived speed of optic flow. *Perception* 27 (1998), 147–148.

40. Laura C Trutoiu, Betty J Mohler, Jörg Schulte-Pelkum, and Heinrich H Bülthoff. 2009. Circular, linear, and curvilinear vection in a large-screen virtual environment with floor projection. *Computers & Graphics* 33, 1 (2009), 47–58.

41. Martin Usoh, Ernest Catena, Sima Arman, and Mel Slater. 2000. Using presence questionnaires in reality. *Presence: Teleoperators and Virtual Environments* 9, 5 (2000), 497–503.

42. WG Wright, P DiZio, and JR Lackner. 2005. Vertical linear self-motion perception during visual and inertial motion: more than weighted summation of sensory inputs. *Journal of Vestibular Research* 15, 4 (2005), 185–195.